

Signature of differential rotation in solar disk-integrated chromospheric line emission

K.-H. HASLER, G. RÜDIGER, and J. STAUDE

Astrophysikalisches Institut Potsdam, An der Sternwarte 16, 14482 Potsdam, Germany

Received 2002 February 19; accepted 2002 March 6

Abstract. UARS SOLSTICE data have been subjected to Fourier and wavelet analyses in order to search for the signature of the solar rotation law in the disk-integrated irradiance of UV lines. Lyman- α , Mg II, and Ca II data show a different behaviour. In the SOLSTICE data there are significant temporal variations of the rotation rate of the UV tracers over 5–6 years. Often several distinct rotation periods appear almost simultaneously. Beside the basic period around 27 days there are signals at 32–35 days corresponding to the rotation rate at very high latitudes. For more than 5 years during another period of the solar cycle the rotational behaviour is quite different; there is an indication of differential rotation of active regions in these Ca II ground-based data. The data contain a wealth of information about the solar differential rotation, but it proves difficult to disentangle the effects of the different emitting sources.

Key words: Sun – stars: rotation

1. Introduction

Almost 90 decades ago Schwarzschild & Eberhard (1913) discovered here in Potsdam the emission reversals in the Ca II H & K lines of solar-like stars. They attributed this effect to active regions, similar to those on the Sun, and formulated “It remains to be shown whether the emission lines of the star have a possible variation in intensity analogous to the sunspot period”. This evidence could be presented 65 years later by Wilson (1978). His pioneer work opened a new horizon for activity cycle research with late-type stars. The discovery of temporal variations of the emission in the Ca II line cores due to plage-like active regions gives the possibility to probe dynamo theories of magnetic stellar activity. The spatial resolution achieved in solar research, on the other hand, still provides the required base for calibrating the theory as done, e.g., with the observations of current helicity by Seehafer (1990), Pevtsov, Canfield & Metcalf (1995) and Abramenko, Wang & Yurchishin (1996).

One basic parameter in the theory is the dependence of the rotation rate $\Omega(r, \theta)$ on depth r and latitude θ . For the Sun the rotation in the interior can be derived by helioseismic sounding from the oscillation frequencies of normal modes

(Kosovichev, Schou & Scherrer al. 1997). The dependence on θ in the atmosphere can be directly measured only for the Sun, and even in this case the results remain controversial (Schröter 1985). Different observational methods such as Doppler shift measurements and correlation tracking of various tracers (e.g. sunspot positions and different chromospheric and coronal features) result in different rotation laws. For example, short-lived chromospheric features in Ca II K show the steepest gradient of $\Omega(\theta)$, while long-lived, large-scale features exhibit almost rigid rotation. Antonucci et al. (1979a, 1979b) found that short-lived features of Ca II K₃ rotate at the same rate as the chromospheric plasma, i.e. faster than the photospheric plasma, while long-lived features rotate like the green corona or coronal holes, almost rigid. Both types of features with rather different shapes of $\Omega(\theta)$ may coexist.

It is not exactly known to which height the tracers belong. A discussion in terms of heights of line formation may be misleading, because that concept is usually based on plane-parallel models of the average quiet solar atmosphere and on the assumption of local thermodynamic equilibrium (Livingston et al. 1991). Such assumptions are far from reality in the active chromosphere, where the magnetic field introduces complicated small-scale structures and violent dynamic processes. Measurements of line core emissions integrated over

Correspondence to: Jürgen Staude, jstaude@aip.de

the solar disk (spectral irradiance) result in a complicated spatial averaging over various features emitting at different heights. Nevertheless, we expect some information on different heights or, more strictly speaking, on emission volumes with different characteristic temperatures when observations in different spectral lines are used.

For other stars the disk-integrated intensities (fluxes) are the only available information, and local activity features on the disk such as plages manifest themselves in a modulation of the flux in time due to the rotation and the development of activity complexes over the cycle. Let us assume a more or less unique shape of $\Omega(\theta)$ for a given star and a latitude drift of the activity belts over the cycle, similar to that of the Sun. Then it would be possible to derive a ‘butterfly diagram’ for the star (see, e.g., Donahue & Keil 1995; Hempelmann & Donahue 1997), and a proxy for differential rotation becomes available. Again this can be tested with the Sun, and for this purpose time series of irradiance measurements of the emission cores of the lines H I Ly- α , the same of the sum of the Mg II h & k lines, and of Ca II K will be discussed in the present paper.

The strong chromospheric lines have been chosen because the modulation amplitude is much larger here than in photospheric tracers and therefore easier to discover in flux measurements. Moreover, irradiance in these strong lines is a direct measure of radiative energy losses in outer stellar atmospheres. Unfortunately, details of the time variation depend critically on the geometry of the emitting volume and on the emission mechanisms of the lines, and these properties are more complicated at chromospheric heights. These lines are formed over an extremely large range of temperatures (T) or heights (h) above the visible continuum: in the VAL IIC standard model of the average quiet Sun (Vernazza, Avrett & Loeser 1981) the line centre of Ly- α is formed at a chromospheric $T \approx 2.5 \cdot 10^4$ K at $h \approx 2200$ km, the wings 1 Å distant from the centre at $T \approx 6200$ K in a plateau at $1200 \lesssim h \lesssim 1800$ km. The corresponding values for Mg II k are $h \approx 2050$ km in a steep gradient of $7500 \lesssim T \lesssim 2.3 \cdot 10^4$ K for the central absorption k_3 , while both features k_1 , the secondary absorption minima and inner wings beyond the emission, are formed in the minimum of $T \approx 4170$ K at $h \approx 500$ km. Ca II K₃ arises at $6700 \lesssim T \lesssim 8200$ K at $1800 \lesssim h \lesssim 2000$ km, K₁ at the minimum of T , similar to Mg II k₁.

2. UARS SOLSTICE

Recent irradiance measurements indicated that solar cycle variability is much smaller than previous estimates. While the Sun varies by nearly a factor of two at Lyman- α (121.6 nm), the variations at wavelengths from 120 to 170 nm are less than 20%. From 180 to 300 nm the variability rapidly decreases to less than 1%.

The Solar Stellar Irradiance Comparison Experiment (SOLSTICE) is one of ten instruments on the Upper Atmosphere Research Satellite (UARS). UARS was launched in September 1991 from the Space Shuttle Discovery during the STS-48 mission. The primary scientific objective for the

SOLSTICE program is to make precise and accurate measurements of the solar UV spectral irradiance over the spectral range 119 to 420 nm. It has also the goal of measuring solar variability over arbitrarily long periods, for example, over the duration of the UARS mission that may exceed ten years.

SOLSTICE goals are to measure i) solar variations on all time scales including the solar rotation variability, ii) 11-year solar cycle variations, and iii) long-term solar variations related to climate research (Rottman & Woods 1988; London, Rottman & Woods 1992; Rottman, Woods & Sparn 1993; Woods, Rottman & Ucker 1993).

SOLSTICE has made continuous daily observations of the Sun since October 3, 1991. The primary science product is a daily mean disk-integrated solar UV spectrum, covering roughly 115 nm to 425 nm with a resolution of 1 nm. Besides the daily mean spectra several special products are also available:

- Daily 280.0 nm Mg II emission core/wing ratio (which, being a ratio, is free of the degradation calibration error),
- daily 121.6 nm Ly- α emission, derived by integrating a Gaussian fit to the emission profile, and
- daily 393.3 nm Ca II emission core/wing ratio.

3. Data analysis

We want to analyze the variability of the rotation of the Sun caused by the passage of UV-emitting sources such as large active regions across the surface of the Sun. We are especially interested in changes of the rotational period of activity features, the sources of the flux variations during the solar cycle; such changes are obviously related to the differential rotation of the solar photosphere and chromosphere.

3.1. Available data

We have analyzed the Ly- α version-8 data, which were available from 3 Oct 1991 (UARS mission day 22) to 28 Feb 1998. The quantity reported here is the integrated irradiance of a least-squares Gaussian fit to the daily-merged Ly- α line profile. For Ly- α the continuum contribution is very small relative to the emission peak.

Moreover, we have analyzed the daily Mg II index which is derived from the SOLSTICE daily mean high resolution solar spectrum (sampling interval about 0.075 nm), and is defined as the ratio of the sum of the integrated intensities of the h & k emission lines to the average continuum in the wings. These data are the version-10 data available from 3 Oct 1991 to 31 Apr 1998.

Further we have analyzed the daily 393.3 nm Ca II index which is also derived from the SOLSTICE daily mean high resolution solar spectrum (SOLSTICE level 3BS data set). The definition of this index is similar to that of the daily Mg II index. The daily Ca II index were available from 3 Oct 1991 to 31 Dec 1996.

The SOLSTICE time series have a few gaps and missing days related to satellite problems.

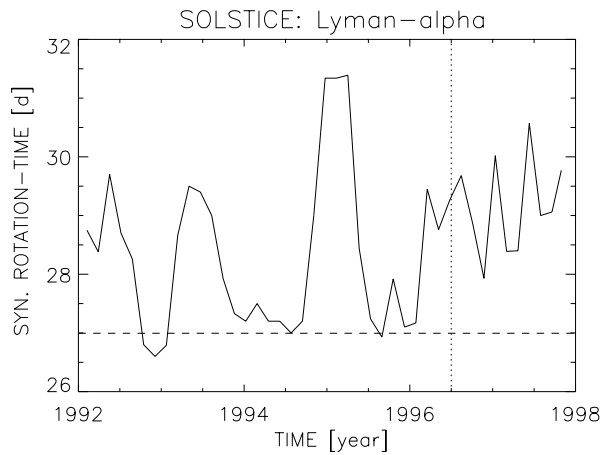


Fig. 1. Mean synodic rotation of the sources of the solar Lyman- α line. The data are from full disk observations by the SOLSTICE experiment aboard the spacecraft UARS from Oct 1991–Feb 1998. The dashed line is the synodic rotation time of the solar surface at the equator. The pointed line is marking the change of the solar cycle. The uncertainty is 0.6d.

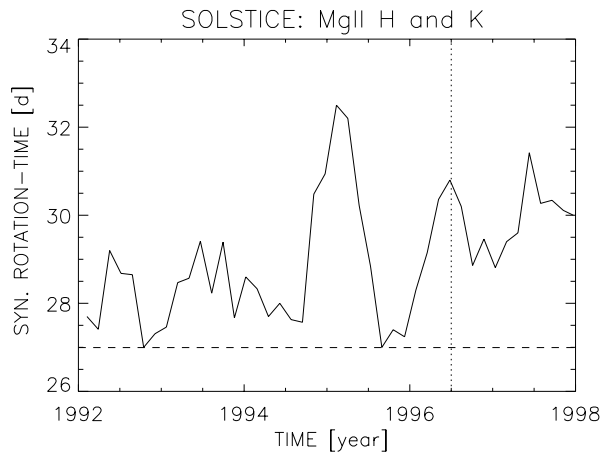


Fig. 2. The same as in Fig. 1, but for the Mg II line from Oct 1991 to Apr 1998.

For comparison and for extending the considered period we have analyzed ground-based full-disk Ca II K data from the Sacramento Peak Observatory (SPO) from Nov 1985 to Mar 1991 by applying similar procedures. The NSO/SPO Ca II K-line monitoring program has been summarized by Keil, Henry & Fleck (1998).

3.2. Fourier analysis

After an extensive treatment of every segment including removal of outliers, a filtering of slow trends by a polynomial fitting, and a high-pass filtering to reduce the influence of low frequency noise, the individual data segments are connected considering their phase. Small gaps are interpolated.

We are interested in the rotation rate and their variability traced by the sources of the UV-emissions in the three lines. Therefore, we have subdivided every time series in overlapping pieces of 256 days, with a difference between the centers

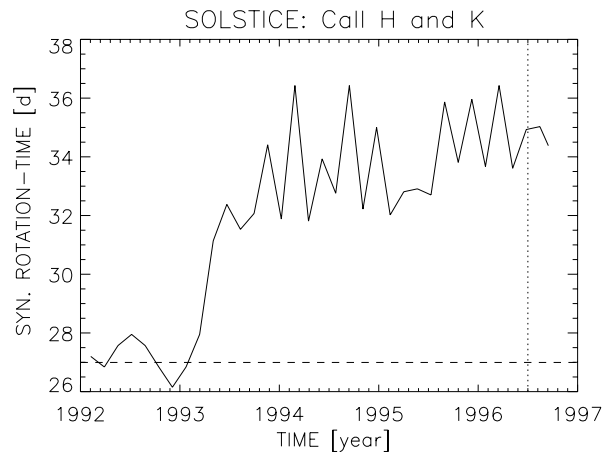


Fig. 3. The same as in Fig. 1 but for the Ca II line from Oct 1991 to Dec 1996.

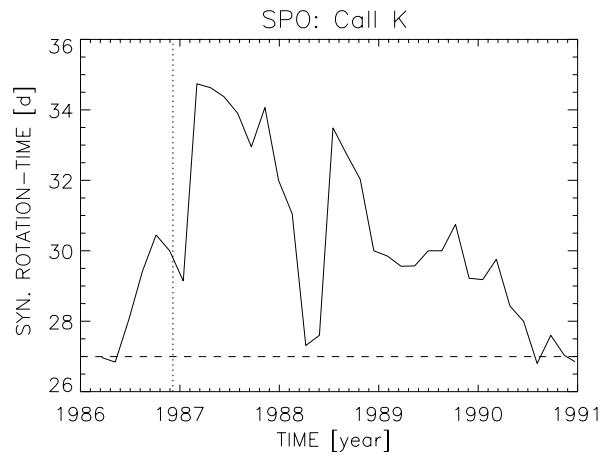


Fig. 4. Mean synodic rotation of the sources of the solar Ca II line. The data are from full disk observations by the Sacramento Peak Observatory from Nov 1985 to Mar 1991. The dashed line is the synodic rotation time of the solar surface at the equator. The pointed line is marking the change of the solar cycle. The uncertainty is 0.6d.

of two neighbouring pieces of 50 days. According to our test calculation this parameter value forms the best compromise between time resolution and frequency resolution.

Then a Fourier analysis of every piece is made, and the frequency of the strongest (assumed as the rotational) peak of every power spectrum is estimated. Because the rotational peaks are relatively broad and in most cases not symmetric, a weighted average of the strongest frequencies around the peak center is formed for the estimate of the center frequency of the peak. The corresponding period is assumed as the rotational period of the sources of the emissions at this point of the time series. Often there are two or more relevant peaks corresponding to different rotational periods. Then also a weighted average of the different periods is assumed as the mean rotational period of the different sources of emission.

Details of the period-time behaviour become visible in a dynamic power spectral analysis by applying a wavelet analysis to the data which has been done as well. For comparison

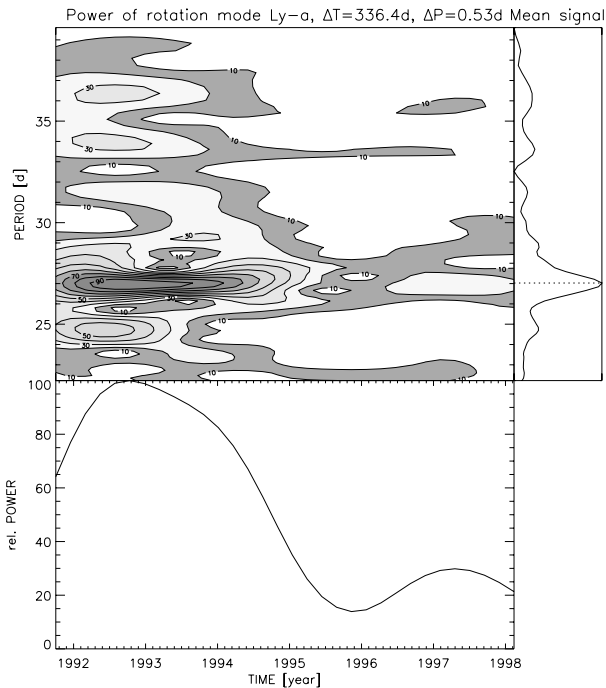


Fig. 5. Wavelet analysis of the SOLSTICE Lyman- α data. The contour lines refer to the power of the transform. The upper right graph shows the time-integrated signal, that is in principle a power spectrum. The lower graph shows the power variations of the maximum, indicated by a dotted line in the upper right graph.

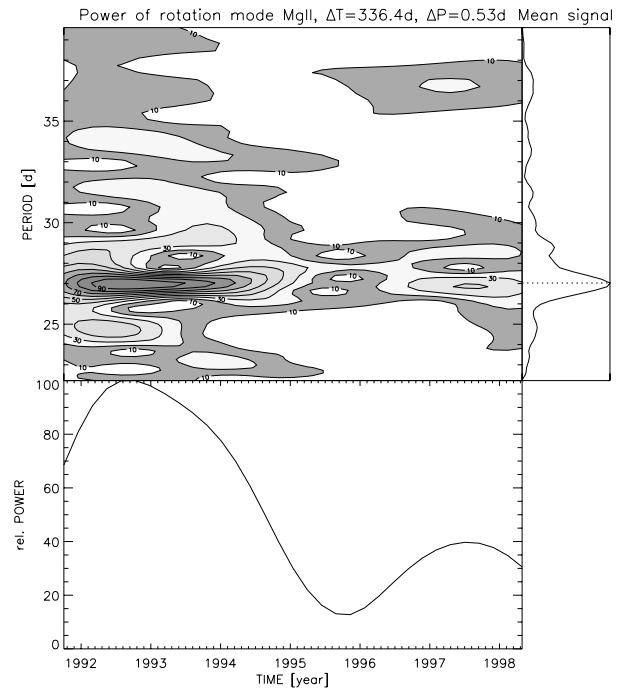


Fig. 6. Wavelet analysis of the SOLSTICE Mg II data

we have performed the analysis for all data sets by applying the same methods.

4. Results

4.1. Power spectra

Early in the UARS mission the Sun was very active, hence the conditions at that time represent solar maximum conditions. There is a very strong and clear signal of the 27-day rotation period of solar variability caused by the passage of large active regions across the disk.

Until solar minimum (middle of 1996), the output of the Sun at UV wavelengths (120 to 420 nm) has continuously decreased. Changes as large as a factor of two are observed at the shortest wavelengths, whereas the changes at the longer, visible wavelengths are only fractions of 1%.

Likewise, the magnitude of the 27-day variations has decreased, but at most of the time a clear signal of the 27-day variability is visible. But also other longer periods are often visible, especially in the last third of the cycle. This effect is very strong in the SOLSTICE CaII data. After the beginning of the current solar cycle the UV emission is increasing again, and also the magnitude of the rotational variations is increasing. The results are shown in Figs. 1–3.

The results for the Ly- α data and the Mg II data are very similar to each other. We find a significant increase of the mean rotation rate at the end of the last (22th) solar cycle and in the beginning of the current (23th) solar cycle. The effect is stronger in the Mg II data.

The Ca II SPO-data show a very strong increase of the rotation time of the sources at the beginning of the new (22th) solar cycle and then a steady decrease in the further progress of the cycle connected with the differential rotation of the solar photosphere and lower chromosphere (Fig. 4). The Ca II SOLSTICE data show a similar behaviour, but the strong increase of the rotation period already starts in the last third of the old (22th) cycle (Fig. 3). Unfortunately, the available data do not allow to analyze the further development. It seems that the different cycles show the same principal features, but a very different behaviour in detail is obvious.

4.2. Wavelet analysis

Sometimes not only one strong peak exists. Often a second or third (strong) peak with smaller frequency corresponding to a longer rotational period appeared especially at the beginning and/or in the end of a solar cycle. At this time sources of the UV-emission were located in regions at different latitudes north and south from the equator taking part in the differential rotation.

A time-period analysis is thus necessary. The results are given in Figs. 5–8. The best compromise between time resolution and frequency resolution is presented. The time resolution should not be shorter than some rotational periods to obtain a signal with a sufficient signal-to-noise ratio.

In the SOLSTICE Ly- α and Mg II data there is a very strong and clear signal of the 27-day rotation period of the Sun variability shortly after the solar maximum caused by the passage of large active regions of the old cycle near the equator. This equatorial signal is then decreasing until the solar minimum and then again increasing. There are also signals with periods of 28–36 days connected with UV-emitting re-

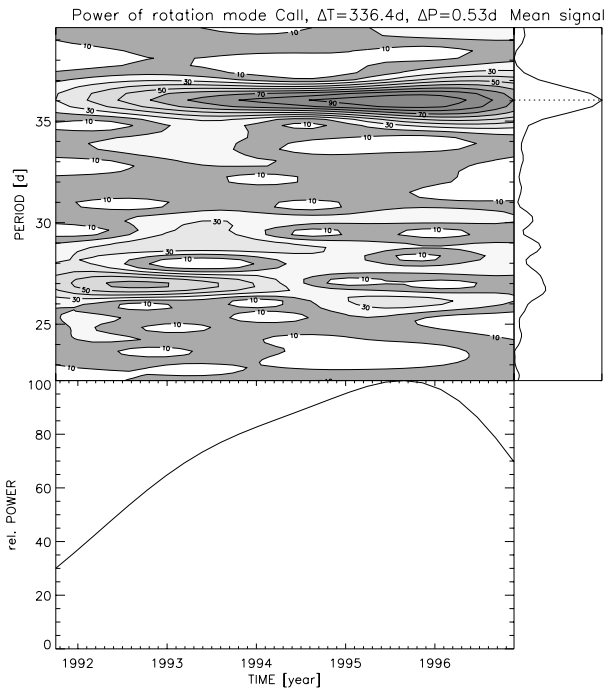


Fig. 7. Wavelet analysis of the SOLSTICE Ca II data.

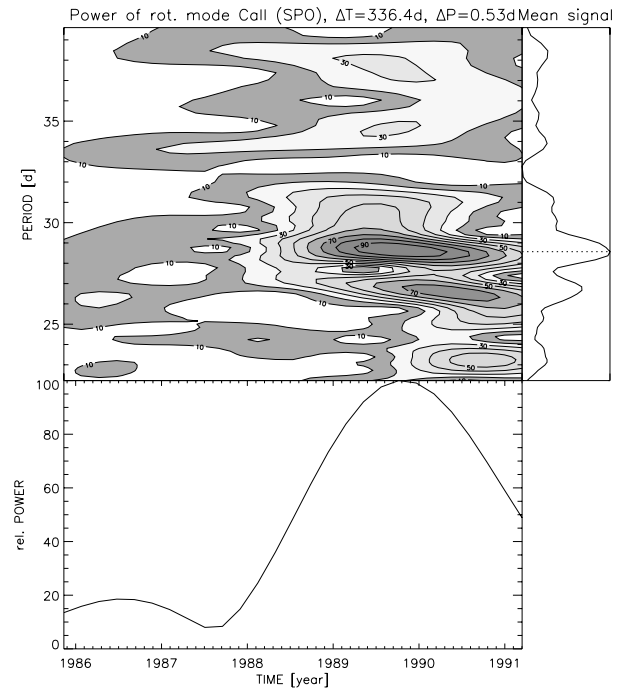


Fig. 8. Wavelet analysis of the SPO Ca II data.

gions of the new cycle located at higher latitudes. They are relatively stronger during the solar minimum and at the beginning of the new (23th) cycle. Also during this time the 36 day signal is stronger marked in the Mg II data than in the Ly- α data (Figs. 5–6).

The results for the SOLSTICE Ca II data (Fig. 7) are somewhat different. The 27-day signal is likewise significant and shows a behaviour similar to that for the Ly- α and Mg II data, but in the end of the old cycle and at the beginning of the new cycle a strong signal with a period around 36 days dominates. This is probably caused by UV emitting sources at high latitudes (70 degree or more), maybe by polar faculae. It is known that in fact the number of polar faculae reaches a maximum early or late in the solar cycle and sometimes even in the solar minimum.

The ground-based Ca II SPO data as reference data show a strong signal 1–2 years after the beginning of the cycle 22, starting with a period of more than 29 days and then decreasing to less than 28 days in the next 2.5 years (Fig. 8). Furthermore, about 2 years after the start of the cycle appears a clear signal starting with a period of 27.5 days and then decreasing nearly to 27 days during the next 2 years. This is a clear signature of differential rotation of the lower chromosphere. It is interesting that weak signals in the high period region around 36 days can also be found at the beginning of the cycle, but they do not occur in the end of the old (21 th) cycle and never dominate.

5. Discussion and conclusions

We have analyzed the disk-integrated emission in 3 solar chromospheric line combinations (HI Ly- α , Mg II h & k, Ca II H & K) measured over several years by the SOLSTICE

instrument on board the UARS satellite and by a ground-based station (Ca II) during another period as well. The ultimate purpose of the present study was to look at the time variations in the emission of certain chromospheric lines for the Sun as a star, integrating over the whole disk, and assuming these variations are the result of the presence and drift of localized active regions, to see if the differential rotation and cycle of activity can be deduced. One would expect these sources to move in latitude as the cycle progresses, perhaps tracing the rotation rate for the locus of the centroid of the activity butterflies. However, this is not exactly what has been found. Instead a number of more complicated and interesting issues arose, having to do with peculiarities of the Sun's chromospheric emission.

There are very large differences between the ground-based (Nov 1985 – Mar 1991) and the SOLSTICE (Oct 1991 – Dec 1996) inferred rotations for Ca II. The rotation of the photosphere varies from 27 days at the equator to about 36 days at the extreme poles. Thus in the Sac Peak (SP) data (Fig. 4), the suggestion is that the sources are at the equator at minimum, then go to high latitudes (but short of the poles) at the start of the new cycle (though the rotation rate is surprisingly low indicating sources way poleward of the activity zone). Then, with a peculiar gap during 1988 (probably due to missing sources at high latitudes), the sources drift toward the equator again and arrive there about solar maximum (now on the equatorward side of the active zone). This time dependence of the rotational period is in general agreement with the results given by Donahue & Keil (1995; their Fig. 3) for the same period, but with a lower resolution in time. More details of the multi-period behaviour become visible in the wavelet data (Fig. 8). In this case the results are similar to those derived by Hempelmann & Donahue (1997; their Fig. 6) for the

period 1987.5 – 1992.0. On the other hand in the SOLSTICE data, the rate drops three years prior to minimum and sometimes appears to be the rate that would be found at very high latitudes, almost at the poles. It seems that the high-latitude activity is far more effective here in producing Ca II emission than the active regions (later and at low latitudes).

Unfortunately, there was no overlap between the available SPO and SOLSTICE data, so that a real comparison between the ground-based and space-borne observations of the UV emission sources could not be made. Therefore the reason for the different cycle-related time dependence seen in Figs. 3–4 and Figs. 7–8 remains somewhat unclear. The wavelet analysis in Figs. 7–8 does not show a single trend that looks like differential rotation $\Omega(\theta)$; instead what it seems to indicate is two different rotation rates where the Ca II emission is strong: the equator and close to the pole — with little in between. During the period 1988.5 – 1991.2 there are two almost parallel bands of enhanced emission with periods ≈ 28.5 and 26.5 days which slowly decrease, pointing out a signature of differential rotation (see also Hempelmann & Donahue 1997; their Fig. 6).

The Lyman- α and Mg II results are similar to each other, but they clearly differ from the Ca II data. Several features in the time dependence of the mean rotational periods (Figs. 1–2) can be explained by looking at the wavelet analysis (Figs. 5–6). In particular, the strong increase of the mean period at the beginning of 1995 (Figs. 1–2) was due to missing emission with a rotational period around 27 days (that means no active regions at low latitudes during the minimum), while there was a weak but dominating emission feature with a period of $P \approx 31 \dots 32$ days. This feature has been identified in the satellite Mg II data from UARS SUSIM as well (Cebula & Deland 1998; their Fig. 7 b). In general the time dependence of the mean rotational periods does not look like differential rotation. However, this conclusion cannot be applied to the details in the wavelet spectra: there is a strong emission with a period of 27 days between 1992 and 1994.5 (active regions close to the equator during the late phase of the cycle), but additionally there appears a strong drift of the period of weaker emission sources from $P \approx 35$ days in 1992 to 27 days in 1996 suggesting the influence of differential rotation.

Generally speaking, the rotation rates of the UV tracers derived from the data show significant variations in time, indicating the influence of differential rotation by the latitudinal drift of the emitting sources over the cycle. But this feature is superimposed by other effects due to a complicated spatial and temporal distribution of different emitting sources such as plages, emerging flux regions, active and enhanced network known from other analyses (see, e.g., Worden, White & Woods 1998). For example, the correlation between Ca II data and a daily plage index has been shown to be smaller in the declining phase of the solar cycle (Keil & Worden 1984). An analysis of the solar mean magnetic field by Mordvinov & Plyusnina (2000) has shown that the rotation and polarity asymmetry behave different during odd and even 11-yr cycles. The variations could be complicated by a number of further effects such as different emission-forming mecha-

nisms for the different lines implying different strengths and center-to-limb variations of the contrast or the influence of the formation and decay of the various features with different temporal scales (e.g. active regions, long-lived activity complexes). In any case the time series of disk-integrated irradiance data of UV lines, their wavelet analyses in particular, contain a wealth of information about the solar differential rotation, but it proves difficult to disentangle the effects of the different emitting sources. A lot of comparative studies of spatially resolved and disk-integrated solar data obtained during different phases of the solar cycle (for Ca II K see, e.g., the work by Worden et al. 1988) remains still to be done. Only then the method can be applied to other late-type stars in order to derive unambiguously the differential rotation law from the temporal variation of spectral irradiance.

Acknowledgements. The critical comments and suggestions by an anonymous referee helped to improve an earlier version of this paper. The authors gratefully acknowledge support of the present work by the German Federal Ministry of Education and Research through the German Space Research Center DLR under grant No. 50 QL 9601 9.

References

- Abramenko, V.I., Wang, T.J., Yurchishin, V.B.: 1996, *SoPh* 168, 75
 Antonucci, E., Doderio, M.A., Thomas, J.H.: 1979a, *SoPh* 62, 107
 Antonucci, E., Azzarelli, L., Casalini, P., Cerri, S., Denoth, F.: 1979b, *SoPh* 63, 17
 Cebula, R.P., Deland, M.T.: 1998, *SoPh* 177, 117
 Donahue, R.A., Keil, S.L.: 1995, *SoPh* 159, 53
 Hempelmann, A., Donahue, R.A.: 1997, *A&A* 322, 835
 Keil, S.L., Henry, T.W., Fleck, B.: 1998, in: K.S. Balasubramaniam, J.W. Harvey, D.M. Rabin (eds.), *Synoptic solar physics*, ASP Conf. Ser. 140, 301
 Keil, S.L., Worden, J.R.: 1984, *ApJ* 276, 766
 Kosovichev, A.G., Schou, J., Scherrer, P.H., et al.: 1997, *SoPh* 170, 43
 Livingston, W., Donnelly, R.F., Grigoryev, V., et al.: 1991, in: A.N. Cox, W.C. Livingston, M.S. Matthews (eds.), *Solar Interior and Atmosphere*, University of Arizona Press, Tucson, p. 1109
 London, J., Rottman, G.J., Woods, T.N.: 1992, in: S. Keevallik, O. Kärner (eds.), *Proc. IRS '92: Current Problems in Atmospheric Radiation*, A. Deepak Publishing, Hampton, Virginia (Ultraviolet Irradiance Derived from SOLSTICE (UARS) Observations)
 Pevtsov, A.A., Canfield, R.C., Metcalf, T.R.: 1995, *ApJ* 440, L 109
 Rottman, G.J., Woods, T.N.: 1988, *SPIE* 924, 136
 Rottman, G.J., Woods, T.N., Sparn, T.P.: 1993, *JGR* 98 (10), 667
 Schröter, E.H.: 1985, *SoPh* 100, 141
 Schwarzschild, K., Eberhard, G.: 1913, *ApJ* 38, 292
 Seehafer, N.: 1990, *SoPh* 125, 219
 Sheely jr., N.R.: 1964, *ApJ* 140, 731
 Stix, M.: 1974, *A&A* 37, 121
 Vernazza, J.E., Avrett, E.H., Loeser, R.: 1981, *ApJS* 45, 635
 Wilson, O.R.: 1978, *ApJ* 226, 379
 Woods, T.N., Rottman, G.J., Ucker, G.: 1993, *JGR* 98 (10), 679
 Worden, J.R., White, O.R., Woods, T.N.: 1998, *ApJ* 496, 998